TIME DILATION IN TYPE Ia SUPERNOVA SPECTRA AT HIGH REDSHIFT[1]

S. Blondin,[2] T. M. Davis,[3,4] K. Krisciunas,[5] B. P. Schmidt,[6] J. Sollerman,[3] W. M. Wood-Vasey,[2] A. C. Becker,[7] P. Challis,[2] A. Clocchiatti,[8] G. Damke,[9] A. V. Filippenko,[10] R. J. Foley,[10] P. M. Garnavich,[11] S. W. Jha,[12] R. P. Kirshner,[2] B. Leibundgut,[13] W. Li,[10] T. Matheson,[14] G. Miknaitis,[15] G. Narayan,[16] G. Pignata,[17] A. Rest,[9,16] A. G. Riess,[18,19] J. M. Silverman,[10] R. C. Smith,[9] J. Spyromilio,[13] M. Stritzinger,[3,20] C. W. Stubbs,[2,16] N. B. Suntzeff,[5] J. L. Tonry,[21] B. E. Tucker,[6] and A. Zenteno[22]

ABSTRACT

We present multiepoch spectra of 13 high-redshift Type Ia supernovae (SNe Ia) drawn from the literature, the ESSENCE and SNLS projects, and our own separate dedicated program on the ESO Very Large Telescope. We use the Supernova Identification (SNID) code of Blondin & Tonry to determine the spectral ages in the supernova rest frame. Comparison with the observed elapsed time yields an apparent aging rate consistent with the $1/(1+z)$ factor (where z is the redshift) expected in a homogeneous, isotropic, expanding universe. These measurements thus confirm the expansion hypothesis, while unambiguously excluding models that predict no time dilation, such as Zwicky's "tired light" hypothesis. We also test for power-law dependencies of the aging rate on redshift. The best-fit exponent for these models is consistent with the expected $1/(1+z)$ factor.

Subject headings: cosmology: miscellaneous — supernovae: general

1. INTRODUCTION

The redshift, z, is a fundamental observational quantity in Friedman-Lemaître-Robertson-Walker (FLRW) models of the universe. It relates the frequency of light emitted from a distant source to that detected by a local observer by a factor $1/(1+z)$. One important consequence is that the observed rate of any time variation in the intensity of emitted radiation will also be proportional to $1/(1+z)$ (see Weinberg 1972 and Appendix A).

Due to their large luminosities (several billion times that of the sun) and variability on short timescales ($\sim$ 20 d from explosion to peak luminosity; Riess et al. 1999; Conley et al. 2006), Type Ia supernovae (SNe Ia) are ideally suited to probe these time-dilation effects across a large fraction of the observable universe. The suggestion to use supernovae as "cosmic clocks" was proposed by Wilson more than six decades ago (Wilson 1939) and tested on light curves of low-redshift SNe Ia in the mid-1970s (Rust 1974), but only since the mid-1990s has this effect been unambiguously detected in the light curves of high-redshift objects (Leibundgut et al. 1996; Goldhaber et al. 2001).

These latter studies show that the light curves of distant SNe Ia are consistent with those of nearby SNe Ia whose time axis is dilated by a factor $(1+z)$. However, there exists an intrinsic variation in the width of SN Ia light curves which is related to their peak luminosities (Phillips 1993), such that more luminous SNe Ia have broader light curves (Fig. 1). This "width-luminosity" relation is derived using low-redshift SNe Ia where the time-dilation effect, if any, is negligible (Phillips 1993; Hamuy et al. 1995; Riess et al. 1995; Phillips et al. 1999; Jha et al. 2007).

It is problematic to disentangle this intrinsic variation of light-curve width with luminosity and the effect of time

[1] Based on observations made with ESO Telescopes at the Paranal Observatory under programs 67.A-0361, 267.A-5688, 078.D-0383, and 080.D-0477; at the Gemini Observatory and NOAO, which are operated by the Association of Universities for Research in Astronomy, Inc., under cooperative agreements with the NSF; with the Magellan Telescopes at Las Campanas Observatory; and at the W. M. Keck Observatory, which was made possible by the generous financial support of the W. M. Keck Foundation.

[2] Harvard-Smithsonian Center for Astrophysics, 60 Garden Street, Cambridge, MA 02138; sblondin@cfa.harvard.edu

[3] Dark Cosmology Centre, Niels Bohr Institute, University of Copenhagen, Juliane Maries Vej 30, DK–2100 Copenhagen Ø, Denmark.

[4] Department of Physics, University of Queensland, QLD, 4072, Australia.

[5] Department of Physics, Texas A&M University, College Station, TX 77843-4242.

[6] The Research School of Astronomy and Astrophysics, The Australian National University, Mount Stromlo and Siding Spring Observatories, via Cotter Road, Weston Creek, PO 2611, Australia.

[7] Department of Astronomy, University of Washington, Box 351580, Seattle, WA 98195-1580.

[8] Pontificia Universidad Católica de Chile, Departamento de Astronomía y Astrofísica, Casilla 306, Santiago 22, Chile.

[9] Cerro Tololo Inter-American Observatory, National Optical Astronomy Observatory, Casilla 603, La Serena, Chile.

[10] Department of Astronomy, University of California, Berkeley, CA 94720-3411.

[11] Department of Physics, University of Notre Dame, 225 Nieuwland Science Hall, Notre Dame, IN 46556-5670.

[12] Department of Physics and Astronomy, Rutgers University, 136 Frelinghuysen Road, Piscataway, New Jersey 08854.

[13] European Southern Observatory, Karl-Schwarzschild-Strasse 2, D-85748 Garching, Germany.

[14] National Optical Astronomy Observatory, 950 North Cherry Avenue, Tucson, AZ 85719-4933.

[15] Fermilab, P.O. Box 500, Batavia, IL 60510-0500.

[16] Department of Physics, Harvard University, 17 Oxford Street, Cambridge, MA 02138.

[17] Departamento de Astronomía, Universidad de Chile, Casilla 36-D, Santiago, Chile.

[18] Johns Hopkins University, 3400 North Charles Street, Baltimore, MD 21218.

[19] Space Telescope Science Institute, 3700 San Martin Drive, Baltimore, MD 21218.

[20] Las Campanas Observatory, Carnegie Observatories, Casilla 601, La Serena, Chile.

[21] Institute for Astronomy, University of Hawaii, 2680 Woodlawn Drive, Honolulu, HI 96822.

[22] Department of Astronomy, University of Illinois at Urbana-Champaign, 1002 West Green St, Urbana, IL 61801-3080.

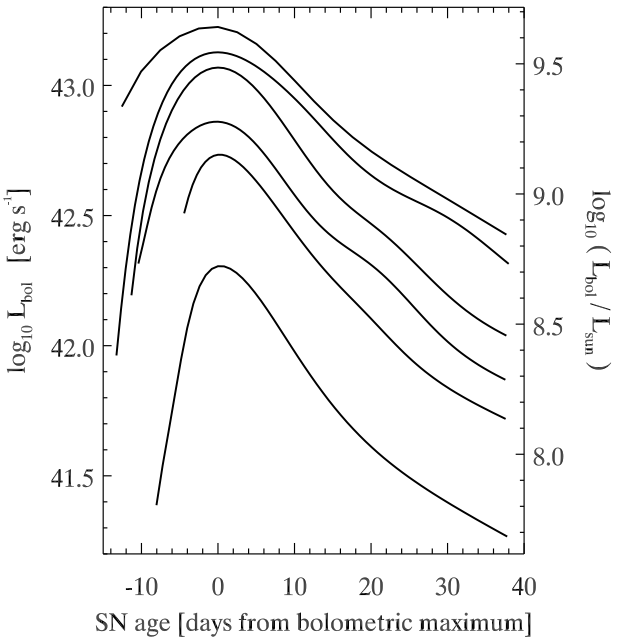

FIG. 1.— Bolometric light curves of 5 low-redshift SNe Ia taken from Stritzinger (2005) (from top to bottom: SNe 1991T, 1999ee, 1994D, 1992A, 1993H, and 1991bg). More luminous SNe Ia have broader light curves. SN 1991bg is an example of intrinsically subluminous SNe Ia (maximum $L_{\rm bol} < 10^9 L_{\rm sun}$), which are less likely to be found at high redshifts.

dilation. To directly test the time-dilation hypothesis one needs to accurately know the distribution of light-curve widths at $z \approx 0$ and its potential evolution with redshift, whether due to a selection effect (not taken into account by Goldhaber et al. 2001) or an evolution of the mean properties of the SN Ia sample with redshift— as possibly observed by Howell et al. (2007). Moreover, one needs to probe sufficiently high redshifts ($z \gtrsim 0.4$, as done by Leibundgut et al. 1996; Goldhaber et al. 2001) such that the observed widths of the SN Ia light curves are broader than the intrinsic width of any nearby counterpart.

Furthermore, one might argue that at high redshift we are preferentially finding the brighter events (akin to a Malmquist bias). Such a selection effect would produce a spurious relation in which there would be broader light curves at higher redshifts, without any time dilation.

The spectra of SNe Ia provide an alternative and a more reliable way to measure the apparent aging rate of distant objects. Indeed, the spectra of SNe Ia are remarkably homogeneous at a given age, such that the age of a SN Ia can be determined from a single spectrum with an accuracy of 1–3 d— with no reference to its corresponding light curve (Riess et al. 1997; Howell et al. 2005; Blondin & Tonry 2007). More importantly, the spectra of SNe Ia spanning a range of luminosities (and hence different intrinsic light-curve widths) evolve uniformly over time (Matheson et al. 2008). The use of spectra thus avoids the degeneracy between intrinsic light-curve width and time-dilation effects. While there are some notable examples of deviations from homogeneity in several SNe Ia (e.g., SN 2000cx, Li et al. 2001a; SN 2002cx, Li et al. 2003; SN 2002ic, Hamuy et al. 2003; SN 2003fg, Howell et al. 2006; SN 2006gz, Hicken et al. 2007), these outliers are readily identifiable spectroscopically through comparison with a large database of supernova spectra (see Section 2 and Blondin & Tonry 2007).

As of today there are two published examples of aging rate measurements using spectra of a single SN Ia (SN 1996bj at $z = 0.574$, Riess et al. 1997; SN 1997ex at $z = 0.362$, Foley et al. 2005). In both cases, the null hypothesis of no time dilation is excluded with high significance ($> 95\%$).

In this paper we present data on 13 high-redshift ($0.28 \leq z \leq 0.62$) SNe Ia for which we have multiepoch spectra. We use the Supernova Identification (SNID) code of Blondin & Tonry (2007) to infer the age of each spectrum in the supernova rest frame, from which we determine the apparent aging rate of each SN Ia. These aging rate measurements are then used to test the $1/(1+z)$ time-dilation hypothesis expected in an expanding universe. The data enable us for the first time to directly test the time-dilation hypothesis *over a large redshift range*.

This paper is organized as follows. In Section 2 we explain how one can determine the age of a SN Ia based on a single spectrum and present the SNID algorithm used for this purpose. The aging rate measurements are presented in Section 3, and the time-dilation hypothesis (amongst others) is tested against the data in Section 4, with the help of model selection statistics (information criteria). Conclusions follow in Section 5.

2. DETERMINING THE AGE OF A SN Ia SPECTRUM

2.1. *SN Ia Spectral Evolution*

The spectra of SNe Ia consist of blended spectral lines, with a profile shape characteristic of stellar outflows. This line profile (also known as a "P Cygni" profile) consists of an emission component symmetric about the line center, and an absorption component that is blueshifted by the $\sim 10,000$ km s^{-1} expansion velocity of the SN ejecta (Pinto & Eastman 2000). The expansion also causes a Doppler broadening of both components, such that a typical spectroscopic feature in SN Ia spectra has a width of ~ 100 Å. As the ejecta expand, the photosphere recedes in the comoving frame of the supernova, such that the spectra probe deeper layers of the ejecta with time. Given the homologous nature of the expansion (velocity proportional to radius), and the chemical stratification in the SN ejecta (Nomoto et al. 1984; Stehle et al. 2005; Mazzali et al. 2008), deeper layers correspond to lower expansion velocities and an increased abundance of iron-peak elements. The impact on the spectra is twofold. First, the blueshift of SN Ia spectral lines decreases with time (by as much as ~ 1000 km s^{-1} per day; Benetti et al. 2005; Blondin et al. 2006). Second, due to the varying chemical composition at the photosphere, the relative shapes and strengths of spectral features change on a timescale of days.

This complex spectral evolution is nonetheless predictable to a large extent. At a given age, the spectra are remarkably homogeneous among different "normal" SNe Ia. According to Li et al. (2001b), these constitute $\sim 65\%$ of the local SN Ia sample, the rest consisting of intrinsically subluminous ($\sim 15\%$) or overluminous ($\sim 20\%$) events, whose spectra show deviations from those of normal SNe Ia. Subluminous SNe Ia are less likely to be found at high redshifts; in fact, no such object has been spectroscopically confirmed in any high-redshift supernova search to this day (e.g., Matheson et al. 2005; Howell et al. 2005). In what follows we only consider

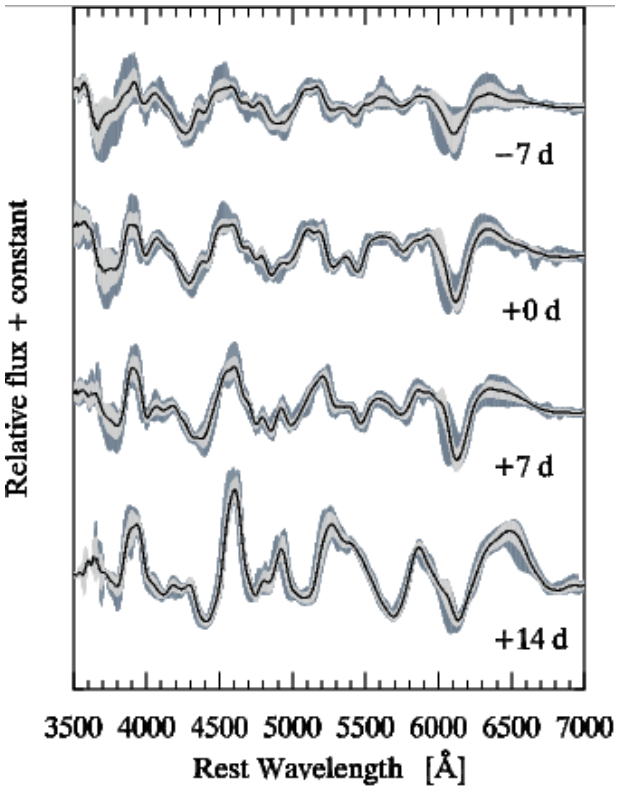

FIG. 2.— Standard (light gray) and maximum (dark gray) deviation from the mean spectrum (black line) for the 22 low-redshift SNe Ia for which we report an aging rate measurement (see Section 4), at four different ages — given in days from B-band maximum light. A low-order curve has been divided out from each spectrum to reveal the relative shapes and strengths of the various spectroscopic features.

normal and overluminous SNe Ia. In a separate paper we will show that none of the SNe Ia in the high-redshift sample presented here (see Section 4) has a spectrum or light curve consistent with the subluminous variety of SNe Ia.

The spectroscopic homogeneity of SNe Ia holds even when we consider both normal and overluminous objects in a representative sample of nearby events. In Fig. 2 we show the mean spectrum for the 22 low-redshift SNe Ia for which we report an aging rate measurement (see Section 4), at four different ages. While there is an intrinsic spectral variance among these different SNe Ia — some spectroscopic features correlate with luminosity (e.g., Nugent et al. 1995; Matheson et al. 2008), the average deviations from the mean spectrum are small, and all spectra evolve in a similar manner over the course of several days, *independent of light-curve width*.

Both the homogeneity and rapid evolution of SN Ia spectra enables an accurate determination of the age of a single spectrum. We explain how this is achieved in practice in the following section.

2.2. *The SNID Algorithm*

Given a large database of finely time-sampled SN Ia spectral templates, we can determine the age of a given input spectrum by finding the best-match template(s) in the database. There are several standard techniques to do this (see Blondin & Tonry 2007 for a review). In this paper, we use an implementation of the correlation techniques of Tonry & Davis (1979): SNID (Blondin & Tonry 2007). SNID automatically determines the type, redshift, and age of a supernova spectrum. We refer the reader to that paper for a more detailed discussion.

The redshift of the input spectrum is a free parameter in SNID, although it can be fixed to a specific value. Comparison of the SNID redshifts with those determined from narrow emission and absorption lines in the host-galaxy spectra (typically accurate to $\lesssim 100$ km s^{-1}; see Falco et al. 1999) yields a dispersion about the one-to-one correspondence of only $\sigma_z \approx 0.005$ out to a redshift $z \approx 0.8$ (Blondin & Tonry 2007).

Similarly, comparison of the SNID ages with those determined using the corresponding light curves yields a typical accuracy < 3 d, comparable to other algorithms (Riess et al. 1997; Howell et al. 2005). However, the age error is systematically overestimated. In this paper, we estimate the error as follows: each spectrum in the SNID database is trimmed to match the rest-frame wavelength range of the input spectrum, and is correlated with all other spectra in the database (except those corresponding to the same supernova). The age error is then given by the mean variance of all template spectra whose SNID age is within one day of the initial estimate.

The success of SNID and similar algorithms lies primarily in the completeness of the spectral database. In Fig. 3 we show the age distribution of the SN Ia templates used in SNID for this paper (these do not include subluminous SNe Ia). This database comprises 959 spectra of 79 low-redshift ($z \lesssim 0.05$) SNe Ia with ages between -15 and $+50$ d from maximum light. The spectra are taken from the literature, from public databases (such as SUSPECT[23] or the CfA Supernova Archive[24]), or from a set of unpublished spectra from the CfA Supernova Program. A full reference to all spectra in the SNID database is given by Blondin & Tonry (2007). It is important to note that each template spectrum is shifted to zero redshift and that each template age is corrected for the expected $(1+z)$ time-dilation factor. Because all the template SNe Ia are at low redshift ($z \lesssim 0.05$), this is a very small correction, and we will see in Section 4 that this has no impact on the aging rate measurements. Thus, SNID determines the age a supernova would have at $z = 0$ — that is, *in the supernova rest frame*.

The number of SNe Ia shown in Fig. 3 is large enough that we can select a subsample (shown as an open histogram) on which to conduct age determinations and aging rate measurements on low-redshift SNe Ia. The size of this subsample is set by the requirement that removing it from the SNID database would leave a sufficient number of templates in a given age bin for a reliable age determination (see Blondin & Tonry 2007). It was also chosen to include a sufficient number of intrinsically overluminous SNe Ia: indeed, there are five such SNe Ia (SNe 1997br, 1998ab, 1999dq, 1999gp, and 2001eh) in this subsample, accounting for $\sim 20\%$ by number of objects and spectra. For these specific tests, the templates corresponding to the 22 SNe Ia in this subsample are temporarily removed from the SNID database to avoid biasing the age determination.

We deliberately restrict this subsample to ages between

[23] http://bruford.nhn.ou.edu/~suspect/index1.html
[24] http://www.cfa.harvard.edu/supernova/SNarchive.html

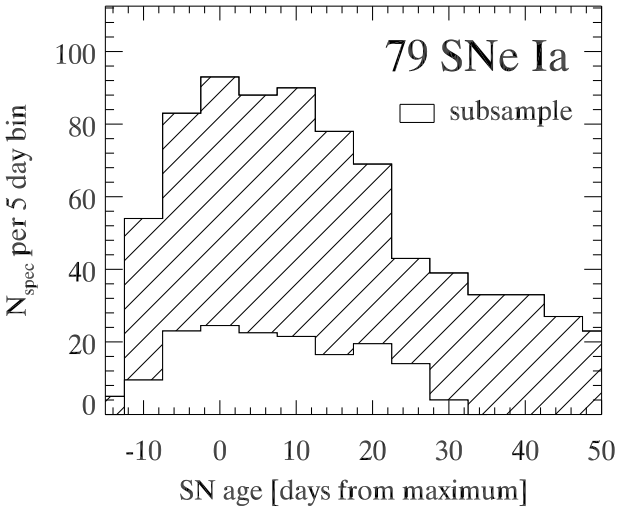

FIG. 3.— Age distribution of the 79 SN Ia templates used in SNID (hatched histogram). There are a total of 959 spectra with ages between −15 and +50 d from B-band maximum light. The open histogram shows the subsample of 145 spectra from 22 SNe Ia (restricted to ages between −10 and 30 d from maximum) for which we report an aging rate measurement (see Section 4).

−10 and +30 d from maximum light. Before −10 d, the number of spectral templates in the SNID database drops rapidly, and the age determination is inaccurate. Past +30 d, the spectra of SNe Ia do not evolve as rapidly as around maximum light, and the age determination is less precise (Blondin & Tonry 2007).

3. AGING RATE AT HIGH REDSHIFTS

3.1. *Spectroscopic Data*

Our aging rate measurements at high redshifts are based on a sample of 35 spectra of 13 SNe Ia in the redshift range $0.28 \leq z \leq 0.62$. These include previously published data by the High-Z Supernova Search Team (SN 1996bj, Riess et al. 1997), the Supernova Cosmology Project (SN 1997ex, Foley et al. 2005; SN 2001go, Lidman et al. 2005), and the ESSENCE project (SNe 2002iz, b027, and 2003js, Matheson et al. 2005). For SN 2001go we present our own reductions of the three epochs of spectroscopic data obtained from the ESO Science Archive Facility[25], as only the first spectrum was published by Lidman et al. (2005). The spectra of SN 04D2an (the highest-redshift SN Ia in this sample) were obtained by members of the Supernova Legacy Survey (SNLS), and will be published as part of a larger sample of SNLS data by Stéphane Basa and coworkers. SN 2006tk will be published alongside the complete ESSENCE supernova dataset in the near future.

The other five SNe Ia (SNe 2006mk, 2006sc, 2007tg, 2007tt, 2007un) are ESSENCE targets which were observed spectroscopically through two dedicated "Target-of-Opportunity" programs at the ESO Very Large Telescope[26].

Details on the instrumental setup and data reduction can be found in the aforementioned references. The rest of the data will be presented more thoroughly in a separate publication. All of the data are shown in Fig. 4.

We use SNID to determine the redshift of each spectrum. The redshift of a given supernova ($z_{\rm SN}$) is then computed as the error-weighted mean of the SNID redshifts ($z_{\rm SNID}$) for each of its spectra (Table 1). For ten SNe Ia, we also have a redshift determination from the host galaxy ($z_{\rm GAL}$). Comparison with the supernova redshift shows an excellent agreement between the two measurements (better than 1%). For the three remaining SNe Ia (SNe b027, 2006tk, and 2007tg), only the SNID redshift is available, but the different redshift measurements for individual spectra all agree to within 1σ, and we are confident about their accuracy. In what follows, we will use the galaxy redshift when available for the age and aging rate measurements. Given the excellent agreement between $z_{\rm GAL}$ and $z_{\rm SN}$, this choice has negligible impact on our results.

[25] http://www.eso.org/sci/archive/ .

[26] Programs 078.D-0383 and 080.D-0477; PI: Jesper Sollerman.

TABLE 1
COMPARISON OF GALAXY AND SUPERNOVA REDSHIFTS

SN (1)	$z_{\rm GAL}$ (2)	$z_{\rm SN}$ (3)	$z_{\rm SNID}$ (4)
1996bj	0.574	0.581 (0.005)	0.580 (0.008)
			0.582 (0.008)
1997ex	0.361	0.362 (0.002)	0.362 (0.005)
			0.361 (0.004)
			0.362 (0.004)
2001go	0.552	0.552 (0.005)	0.552 (0.008)
			0.556 (0.008)
			0.550 (0.009)
2002iz	0.427	0.425 (0.004)	0.422 (0.006)
			0.428 (0.006)
b027	···	0.315 (0.003)	0.315 (0.006)
			0.315 (0.004)
2003js	0.363	0.361 (0.003)	0.359 (0.004)
			0.363 (0.006)
04D2an	0.621	0.614 (0.006)	0.608 (0.007)
			0.625 (0.011)
2006mk	0.475	0.477 (0.003)	0.479 (0.005)
			0.478 (0.007)
			0.474 (0.008)
			0.476 (0.006)
2006sc	0.357	0.356 (0.004)	0.355 (0.007)
			0.357 (0.007)
			0.356 (0.006)
2006tk	···	0.312 (0.003)	0.312 (0.006)
			0.310 (0.003)
			0.315 (0.006)
2007tg	···	0.502 (0.004)	0.503 (0.009)
			0.503 (0.008)
			0.502 (0.007)
2007tt	0.374	0.376 (0.004)	0.367 (0.008)
			0.379 (0.007)
			0.377 (0.005)
2007un	0.283	0.285 (0.004)	0.287 (0.006)
			0.285 (0.007)
			0.285 (0.005)

Column headings: (1) SN name. (2) Galaxy redshift (the typical error is < 0.001). (3) SN redshift, quoted as the error-weighted mean of the individual redshifts for each epoch. (4) SNID redshift for each epoch, in order of increasing age.

3.2. *Accuracy of Relative Age Determination*

An accurate determination of the rate of aging involves accurate knowledge of age *differences*. In what follows we test how well SNID determines differential ages using the subsample of low-redshift SNe Ia presented in Section 2.2. While the determination of *absolute* ages has no impact on the main result of this paper, we discuss their accuracy in Appendix B.

We determine the rest-frame age ($t_{\rm spec}$) of each of the

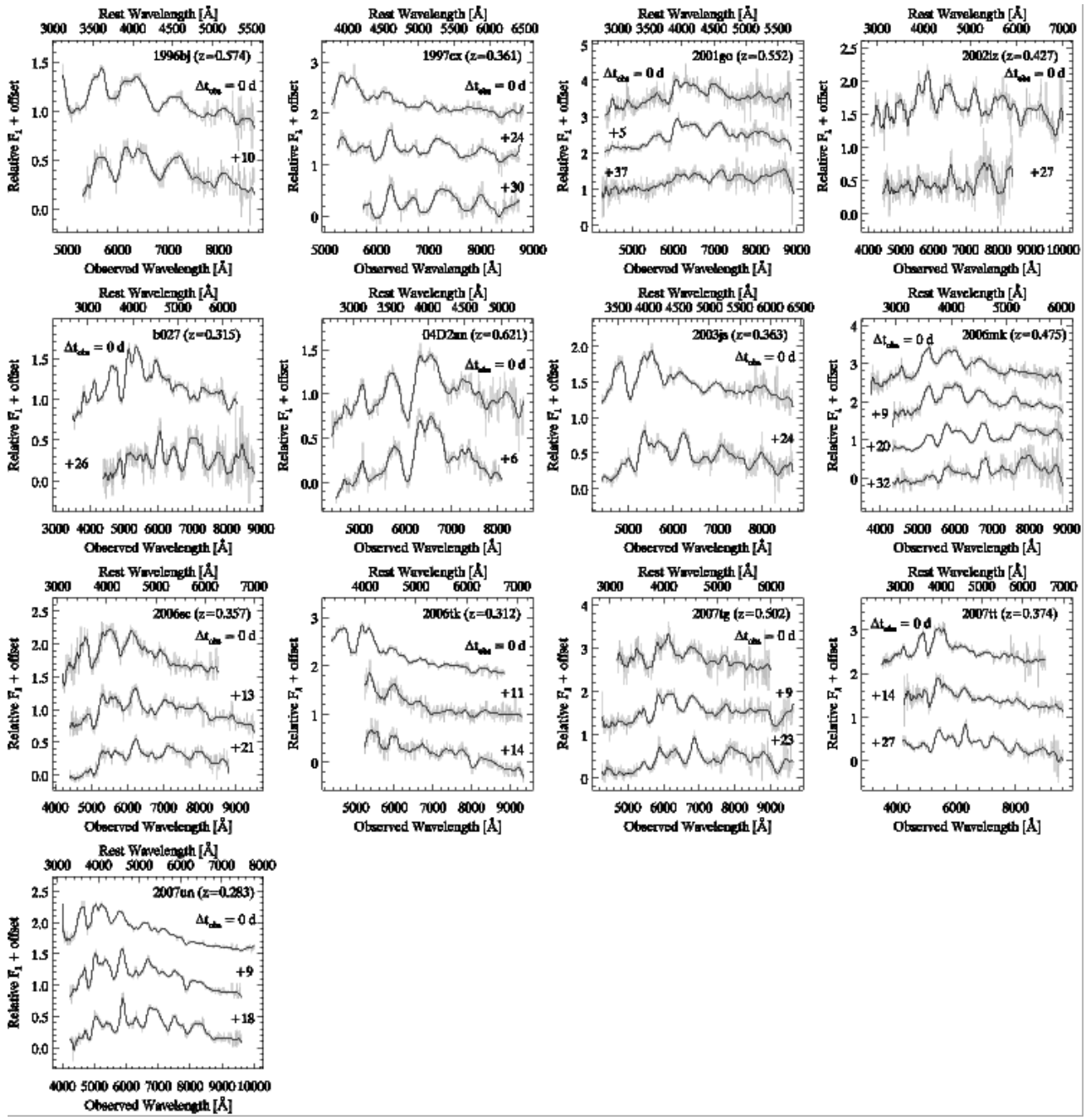

FIG. 4.— Multiepoch spectra of the 13 high-redshift SNe Ia used in this study, binned to 10 Å (gray). The vertical offset between each spectrum is for clarity only, and does not reflect differences in flux density (F_λ; erg s^{-1}cm^{-2}Å^{-1}) between them. In each plot, the age of the supernova increases downwards, and the observed time (in days) from the first spectrum is indicated. Overplotted in black is a smoothed version using the inverse-variance-weighted Gaussian algorithm of Blondin et al. (2006).

145 spectra in the low-redshift subsample of 22 SNe Ia. We then compute the absolute age difference ($\Delta t_{\rm spec}$) between each unique pair of spectra corresponding to a given supernova. This amounts to 631 pairs. This age difference is then compared with the absolute observer-frame age difference ($\Delta t_{\rm obs}$) for each spectrum pair. Since $z \approx 0$ for this subsample, $\Delta t_{\rm spec}$ can be directly compared to $\Delta t_{\rm obs}$ with no correction for time dilation. Given the restriction to ages between -10 and $+30$ d from maximum light in the low-redshift subsample, $\Delta t_{\rm spec}$ (and hence $\Delta t_{\rm obs}$) is at most 40 d.

The results are displayed in the upper panel of Fig. 5. There is good agreement between $\Delta t_{\rm spec}$ and $\Delta t_{\rm obs}$, with a dispersion of only 2.0 d about the one-to-one correspondence. For $\Delta t_{\rm obs} \gtrsim 30$ d, however, SNID systematically underestimates the age difference by ~ 1.5 d. This is more apparent in the plot of residuals in the middle panel. it is mainly due to a systematic overestimate of rest-frame ages $t_{\rm spec} \lesssim -7$ d from maximum light, due to the lack of spectral templates in the SNID database with similar ages (see Fig. 3 and Blondin & Tonry 2007).

The lower panel of Fig. 5 shows the absolute fractional age difference vs. $\Delta t_{\rm obs}$. The quantity $|\Delta t_{\rm obs}/\Delta t_{\rm spec}|$ is a direct measure of the accuracy we can achieve for the aging rate determination. As expected, the fractional age difference decreases with increasing age differ-

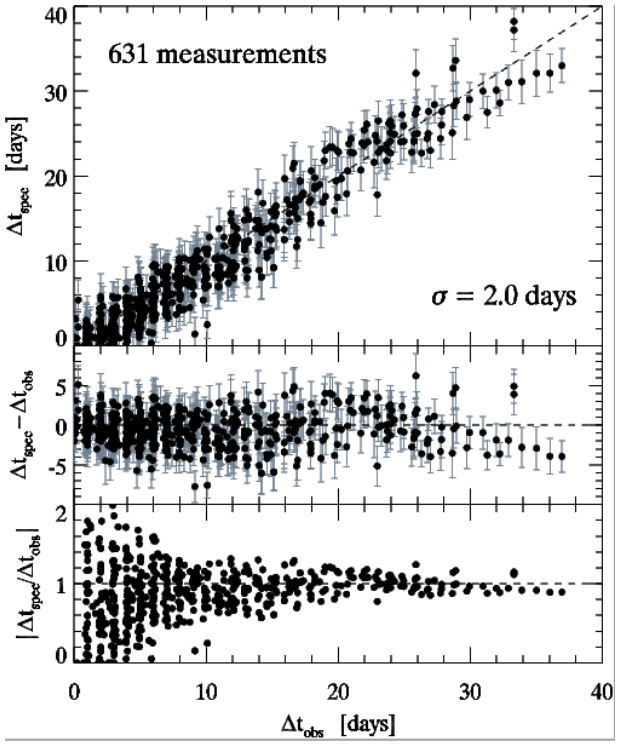

FIG. 5.— Upper panel: Rest-frame age difference ($\Delta t_{\rm spec}$) vs. observer-frame age difference ($\Delta t_{\rm obs}$) for each spectrum pair for a given supernova. There are 631 such pairs, with a dispersion of 2.0 d about the one-to-one correspondence. Middle panel: Residuals in the upper panel vs. $\Delta t_{\rm obs}$. Lower panel: Ratio of $\Delta t_{\rm spec}$ to $\Delta t_{\rm obs}$, again vs. $\Delta t_{\rm obs}$. For $\Delta t_{\rm obs} > 6$ d, the fractional difference is less than 20%.

ence. For $\Delta t_{\rm obs} > 6$ d, this difference drops below 20%. The high-redshift data presented in the previous section span a sufficient range of observer-frame age difference that the aging rate determination is accurate. Note that the systematic underestimate of the age difference for $\Delta t_{\rm obs} \gtrsim 30$ d results in a negligible fractional difference.

3.3. *Aging Rate Determination*

The rest-frame age of each high-redshift SN Ia spectrum ($t_{\rm spec}$) is determined as outlined in Section 2.2. In each case, we fix the redshift to that determined in the previous section. The results are displayed in Table 2, along with the corresponding observed date of each spectrum ($t_{\rm obs}$). However, since the aging rate determination depends on age *differences* (see previous Section), we also report the observer-frame and rest-frame age from the first spectrum, respectively denoted $\Delta t_{\rm obs}$ and $\Delta t_{\rm spec}$ in Table 2.

We can then trivially compute the aging rate for each supernova. This is simply done through a least-squares fit of a line to $\Delta t_{\rm spec}$ versus $\Delta t_{\rm obs}$. The slope of the line is a measure of the aging rate, which should equal $1/(1+z)$ in an expanding universe (see Appendix A). Were there no time dilation, the aging rate would equal one. The results are displayed in Fig. 6.

We note that comparing the inverse of the slope in Fig. 6 (denoted "age factor" by Foley et al. 2005) and $(1+z)$ leads to asymmetric errors. The errors on the "age factor" [$\equiv (1+z)$] become highly non-Gaussian when the uncertainties of the individual age measurements are large ($\gtrsim 1$ d, as is the case in this paper, and in Foley et al. 2005 for SN 1997ex), whereas the errors on the aging rate [$\equiv 1/(1+z)$] are always Gaussian. This is illustrated in Fig. 7 using a Monte Carlo simulation of the age measurements for SN 1997ex presented by Foley et al. (2005). Using the same errors on the individual age measurements, the distribution of the slope measurements is highly non-Gaussian in $(1+z)$ space, while it is normally distributed in $1/(1+z)$ space.

The individual aging rate measurements presented here alone reject models that predict no time dilation at a high significance (up to $\sim 6\sigma$), and all (except for SN 2006mk) are within 1σ of the expected $1/(1+z)$ factor. In the next section we combine all aging rate measurements (including those for the low-redshift sample) to test each hypothesis more thoroughly.

TABLE 2
OBSERVER-FRAME AND REST-FRAME AGE DIFFERENCES

SN (1)	$t_{\rm obs}$ (2)	$t_{\rm spec}$ (3)	$\Delta t_{\rm obs}$ (4)	$\Delta t_{\rm spec}$ (5)
1996bj	367.99	−2.2 (3.0)	0.00	0.0 (3.0)
	378.04	3.1 (2.2)	10.05	5.3 (2.2)
1997ex	815.08	−1.6 (1.6)	0.00	0.0 (1.6)
	839.96	17.4 (2.1)	24.88	19.0 (2.1)
	846.03	21.2 (2.0)	30.95	22.8 (2.0)
2001go	2021.70	7.9 (2.3)	0.00	0.0 (2.3)
	2027.69	9.8 (1.7)	5.99	1.9 (1.7)
	2059.17	31.2 (1.6)	37.47	23.3 (1.6)
2002iz	2586.95	−0.5 (2.2)	0.00	0.0 (2.2)
	2614.57	17.6 (1.2)	27.62	18.1 (1.2)
b027	2589.95	−3.5 (1.8)	0.00	0.0 (1.8)
	2616.57	18.4 (1.6)	26.62	21.9 (1.6)
2003js	2942.46	−4.9 (1.6)	0.00	0.0 (1.6)
	2966.71	12.5 (1.2)	24.25	17.4 (1.2)
04D2an	3026.20	−2.5 (1.6)	0.00	0.0 (1.6)
	3032.20	0.9 (1.3)	6.00	3.4 (1.3)
2006mk	4031.71	−6.2 (1.0)	0.00	0.0 (1.0)
	4040.72	−0.6 (2.2)	9.01	5.6 (2.2)
	4051.77	7.3 (1.9)	20.06	13.5 (1.9)
	4063.78	18.5 (1.8)	32.07	24.7 (1.8)
2006sc	4063.58	0.9 (1.6)	0.00	0.0 (1.6)
	4076.65	9.8 (1.4)	13.07	8.9 (1.4)
	4084.68	13.4 (2.2)	21.10	12.5 (2.2)
2006tk	4089.57	−8.8 (2.4)	0.00	0.0 (2.4)
	4100.57	0.3 (2.0)	11.00	9.1 (2.0)
	4103.59	2.9 (0.9)	14.02	11.7 (0.9)
2007tg	4381.75	−6.1 (2.0)	0.00	0.0 (2.0)
	4391.65	−0.5 (1.8)	9.90	5.6 (1.8)
	4405.61	10.0 (1.5)	23.86	16.1 (1.5)
2007tt	4415.81	−5.0 (2.1)	0.00	0.0 (2.1)
	4430.65	6.1 (1.4)	14.84	11.1 (1.4)
	4443.58	14.9 (2.2)	27.77	19.9 (2.2)
2007un	4441.61	3.2 (2.2)	0.00	0.0 (2.2)
	4451.60	11.1 (1.3)	9.99	7.9 (1.3)
	4460.58	17.7 (1.4)	18.97	14.5 (1.4)

Column headings: (1) SN name. (2) Julian date (JD) minus 2,450,000 at midpoint of observation. (3) SN rest-frame age in days from maximum light, derived from the cross-correlation with spectral templates using SNID. (4) Observer-frame days from first spectrum. (5) Rest-frame days from first spectrum.

4. TESTING THE $1/(1+z)$ TIME-DILATION HYPOTHESIS

We have determined the aging rate for the subsample of 22 low-redshift SNe Ia. We combine these aging rates with those determined for the 13 high-redshift SNe Ia of our sample (see Table 3) to test the $1/(1+z)$ time-dilation hypothesis. As noted in Section 3.2 and Appendix B, these measurements rely on a database of SN Ia spectra whose ages have already been corrected for the expected $1/(1+z)$ time-dilation factor. However, since all SNe Ia

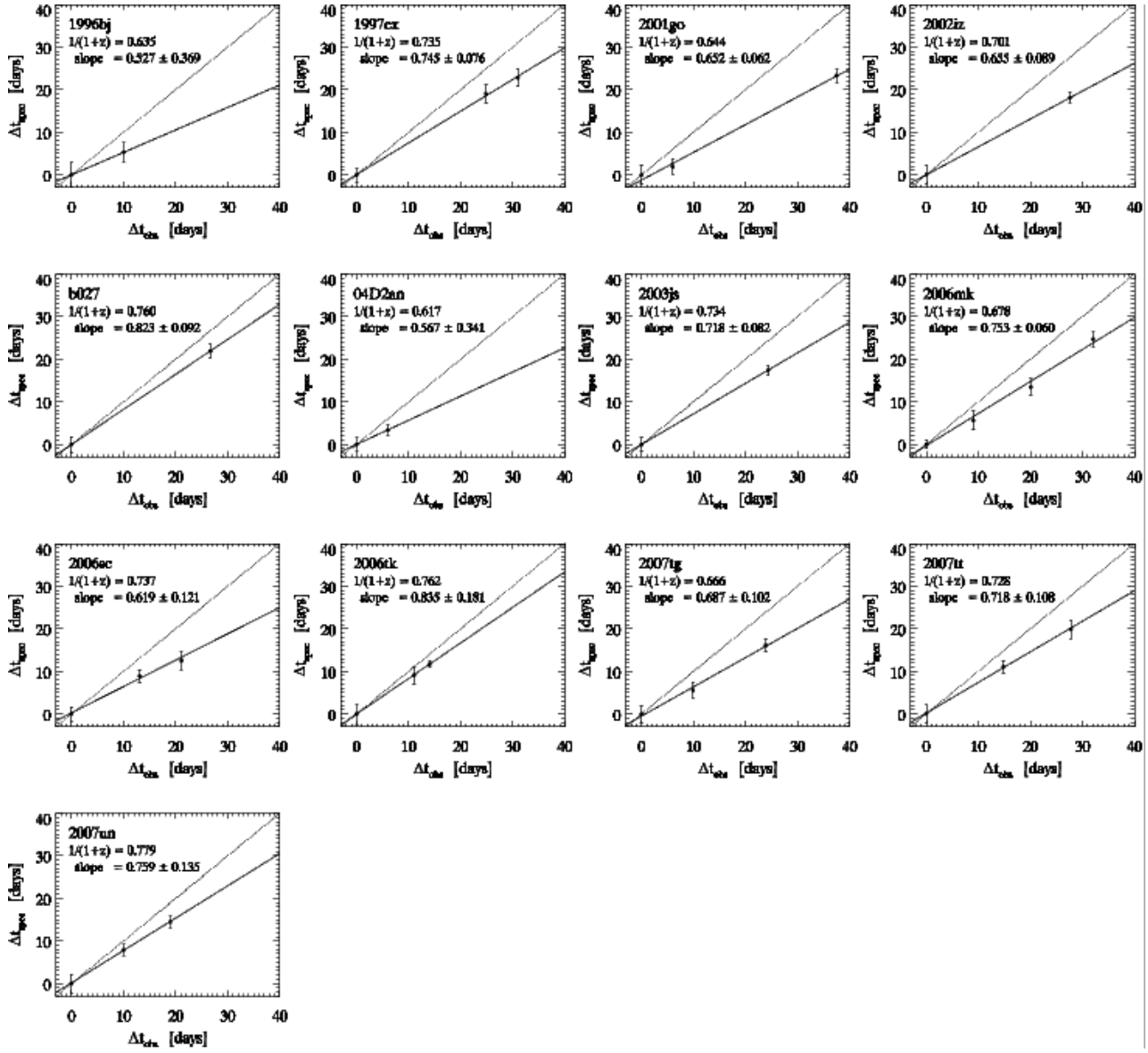

FIG. 6.— Comparison of rest-frame ($\Delta t_{\rm spec}$) and observer-frame ($\Delta t_{\rm obs}$) time from the first spectrum, for each of the 13 high-redshift SNe Ia in our sample. The abscissa and ordinate ranges are both set to [−3,+40] d in all cases. The slope of the best-fit line (solid line) gives a measurement of the apparent aging rate of the supernova, which is compared to the expected $1/(1+z)$ value. The dotted line in each plot corresponds to $\Delta t_{\rm spec} = \Delta t_{\rm obs}$.

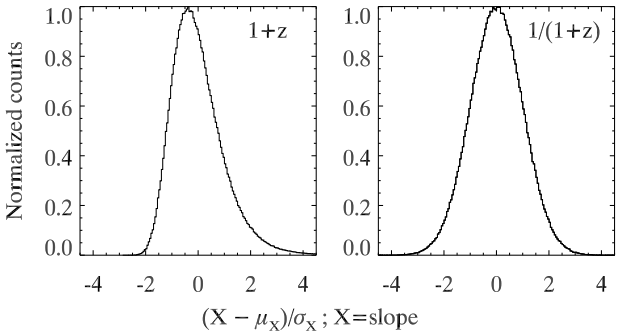

FIG. 7.— Monte Carlo results illustrating the advantage of working in $1/(1+z)$ space for time-dilation measurements. Solid lines: recovered slope (in standard deviations from the mean, μ) in $(1+z)$ (left) and $1/(1+z)$ space (right), using the SN age errors reported by Foley et al. (2005). The distribution is highly non-Gaussian in the former case.

in the SNID database are at redshifts $z \leq 0.05$, the correction is small ($\lesssim 1$ d) and has a negligible impact on the aging rate measurements.

All aging rate measurements are shown in Fig. 8. The solid line shows the expected $1/(1+z)$ time-dilation factor, while the dashed line represents the "tired light" hypothesis of Zwicky (1929). According to this hypothesis, photons lose energy as they interact with matter and other photons in a static universe. The energy loss is proportional to the distance from the source, and causes a redshift in spectra as in an expanding universe. However, this hypothesis does not predict a time-dilation effect, and so the aging rate should equal one for all redshifts.

As expected, the measurement of a time-dilation effect is more obvious at larger redshift, and the precision improves as the number and time span of spectra for each supernova increases. This latter effect explains why the aging rate measurements for SN 1996bj ($z = 0.574$) and SN 04D2an ($z = 0.621$) have a large associated error — despite being the two highest-redshift SNe Ia in our sample, since only two spectra separated by ~ 10 (for

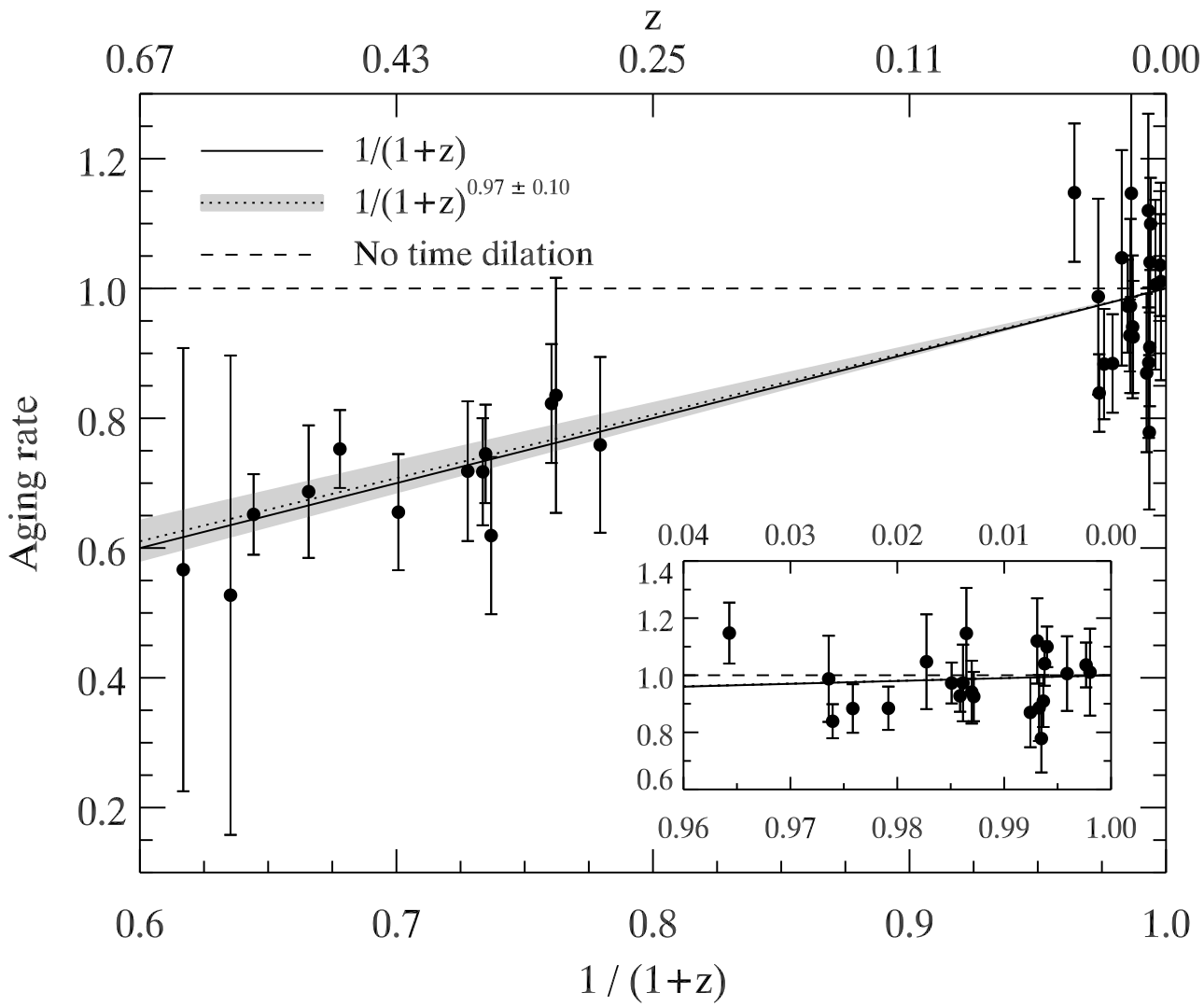

FIG. 8.— Apparent aging rate versus $1/(1+z)$ for the 13 high-redshift ($0.28 \leq z \leq 0.62$) and 22 low-redshift ($z < 0.04$) SNe Ia in our sample. Overplotted are the expected $1/(1+z)$ time dilation (solid line) and the best-fit $1/(1+z)^b$ model (with $b = 0.97 \pm 0.10$; dotted line and gray area). The dashed line corresponds to no time dilation, as expected in the tired-light model — clearly inconsistent with the data. The inset shows a close-up view of the low-redshift sample. These data are summarized in Table 3.

SN 1996bj) and ~ 6 (for SN 04D2an) observer-frame days are available.

A simple χ^2 analysis is sufficient to confirm what the eye sees: the hypothesis of no time dilation is not a good fit to the data ($\chi^2 = 150.3$ for 35 degrees of freedom; see Table 4), with a goodness-of-fit of $\sim 0\%$ (defined as GoF= $\Gamma(\nu/2, \chi^2/2)/\Gamma(\nu/2)$, where $\Gamma(\nu/2, \chi^2/2)$ is the incomplete gamma function and ν is the number of degrees of freedom) — namely, a null probability of obtaining data that are a worse fit to the model, assuming that the model is indeed correct. The expected $1/(1+z)$ time-dilation factor, on the other hand, yields a good fit to the data ($\chi^2 = 27.0$ for 35 degrees of freedom), with GoF= 83.2%, and is largely favored over the null hypothesis of no time dilation ($\Delta\chi^2 \approx 123$).

This result holds (and in fact improves) when we consider only the high-redshift sample (see Table 4). This works because the $z = 0$ end of the aging rate versus redshift relation (Fig. 8) is fixed to unity by theory, so the low-redshift sample is not needed to anchor the theoretical curve at $z \approx 0$ (although it is still used to calibrate the $t_{\rm spec}$ measurement). The low-redshift data alone do not enable us to distinguish between the two hypotheses, since the impact of time dilation is small at such low redshifts.

In Fig. 9 a different view of Fig. 8 shows the distributions of the ratio between the aging rate and $1/(1+z)$ for both the low-redshift (open histogram) and high-redshift (hatched histogram) samples. Both distributions are within $\sim 20\%$ of a unit ratio, again validating the hypothesis of time dilation over a large redshift range. The apparent bias to lower values of the ratio for the low-redshift sample is not statistically significant, as the mean error on the aging rate is of order one bin size ($\lesssim 0.1$; see Table 3).

In what follows we test whether the data favor a nonlinear dependence of the aging rate on redshift, namely

$$\text{aging rate} = \frac{1}{(1+z)^b}, \qquad (1)$$

where b is a free parameter. While Eq. [1] satisfies the same zero point as the two previous hypotheses (aging rate equal to 1 at $z = 0$), no model actually predicts such a dependence of the aging rate on redshift. Nonetheless,

TABLE 3
Aging rate measurements

SN	z	$1/(1+z)$	Aging rate
Low redshift ($z < 0.04$)			
1981B	0.006	0.994	1.099 (0.071)
1989B	0.002	0.998	1.036 (0.079)
1992A	0.006	0.994	1.040 (0.077)
1994D	0.002	0.998	1.011 (0.152)
1996X	0.007	0.993	0.886 (0.116)
1997br	0.007	0.993	1.120 (0.149)
1998V	0.018	0.983	1.047 (0.166)
1998ab	0.027	0.974	0.987 (0.151)
1998dm	0.007	0.993	0.778 (0.119)
1998eg	0.025	0.976	0.883 (0.085)
1999cl	0.008	0.992	0.870 (0.122)
1999dq	0.014	0.986	0.928 (0.055)
1999ej	0.014	0.986	1.147 (0.159)
1999gp	0.027	0.974	0.839 (0.060)
2000fa	0.021	0.979	0.884 (0.076)
2001V	0.015	0.985	0.973 (0.072)
2001eh	0.037	0.964	1.148 (0.107)
2001ep	0.013	0.987	0.925 (0.086)
2002ha	0.014	0.986	0.973 (0.134)
2003cg	0.004	0.996	1.006 (0.131)
2003du	0.006	0.994	0.909 (0.091)
2006lf	0.013	0.987	0.941 (0.110)
High redshift ($z > 0.2$)			
1996bj	0.574	0.635	0.527 (0.369)
1997ex	0.361	0.735	0.745 (0.076)
2001go	0.552	0.644	0.652 (0.062)
2002iz	0.427	0.701	0.655 (0.089)
b027	0.315	0.760	0.823 (0.092)
2003js	0.363	0.734	0.718 (0.082)
04D2an	0.621	0.617	0.567 (0.341)
2006mk	0.475	0.678	0.753 (0.060)
2006sc	0.357	0.737	0.619 (0.121)
2006tk	0.312	0.762	0.835 (0.181)
2007tg	0.502	0.666	0.687 (0.102)
2007tt	0.374	0.728	0.718 (0.108)
2007un	0.283	0.779	0.759 (0.135)

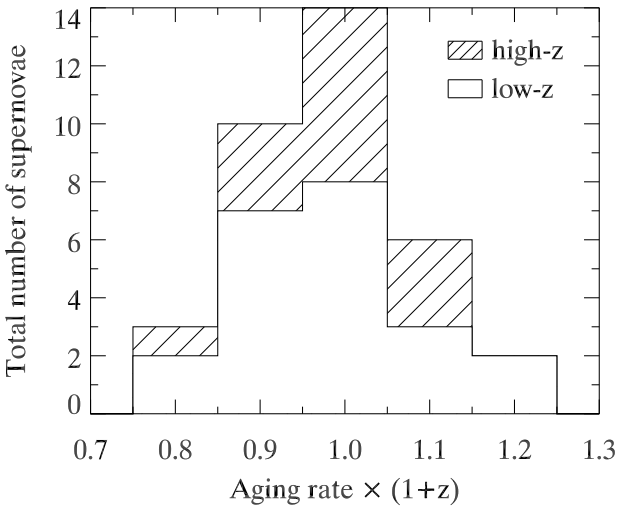

FIG. 9.— Ratio of the aging rate to $1/(1+z)$ for all SNe Ia in Fig. 8. Both the low-redshift (open histogram) and high-redshift (hatched histogram) samples are shown.

small deviations from the expected $1/(1+z)$ factor would have profound implications for our assumption of FLRW cosmology.

Again, we performed a least-squares fit to the entire sample, and also to the individual high- and low-redshift samples (see Table 4). The data constrain the b exponent to 10% (1σ), and yield $b = 0.97 \pm 0.10$ for the entire sample (Fig. 8; dotted line and gray region) and $b = 0.95 \pm 0.10$ for the high-redshift sample. As expected, the low-redshift sample alone is insufficient to constrain the free parameter ($b = 3.18 \pm 1.28$). Nonetheless, the samples that include the high-redshift objects have a best-fit value for b that is consistent with $b = 1$, and thus with the expected $1/(1+z)$ time-dilation factor.

Since this model has an additional free parameter, it is instructive to use information criteria to compare it to the simple $1/(1+z)$ prediction. These model comparison statistics favor models that yield a good fit to the data with fewer parameters. As in Davis et al. (2007), we use the Akaike information criterion (AIC; Akaike 1974). For Gaussian errors (which is the case here, see Section 3.3), this criterion can be expressed as

$$\mathrm{AIC} = \chi^2 + 2k, \tag{2}$$

where k is the number of free parameters (Davis et al. 2007). Comparison of models simply involves computing the difference in AIC (ΔAIC) with respect to the model with the lowest value for this criterion. A difference in AIC of 2 is considered positive evidence against the model with the higher AIC, whereas a difference of 6 is considered strong evidence (Liddle 2004; Davis et al. 2007). In the models considered here (see Table 4), the expected $1/(1+z)$ time-dilation model has the lowest AIC (although this is not true for the low-redshift sample), and we compute AIC differences with respect to that model.

With $\Delta\mathrm{AIC} = 1$, we conclude that the information criteria do not provide positive evidence against a $1/(1+z)^b$ dependence of the aging rate. The χ^2 per degree of freedom is also satisfactory for the samples that include the high-redshift objects.

The two other models considered previously have no free parameters ($k = 0$ in Eq. [2]), hence $\Delta\mathrm{AIC} = \Delta\chi^2$, and the information criterion is reduced to a simple χ^2 test.

5. CONCLUSION

We have presented 35 spectra of 13 high-redshift ($0.28 \leq z \leq 0.62$) SNe Ia, which include previously unpublished data from the ESSENCE and SNLS projects and from our own dedicated program at the ESO Very Large Telescope. Given the rapid and predictable evolution of SN Ia spectral features with age, as well as the relative homogeneity of SN Ia spectra at a given age, one is able to determine the (rest-frame) age of a single spectrum with a typical accuracy of 1–3 d (Riess et al. 1997; Foley et al. 2005; Hook et al. 2005; Howell et al. 2005; Blondin & Tonry 2007).

Using the Supernova Identification (SNID) code of Blondin & Tonry (2007), we determine the ages of each spectrum in the supernova rest frame. Comparison with the observed time difference between the spectra yields an apparent aging rate consistent with $1/(1+z)$, as expected in a homogeneous and isotropic expanding universe. Moreover, the data unambiguously rule out the "tired light" hypothesis (Zwicky 1929) in which photons lose energy as they interact with matter and other photons in a static universe.

The fact that the age determination is so accurate over a large redshift range also shows that the deviations be-

TABLE 4
Time-dilation model comparison

Model[a]	All SNe			High-redshift SNe only			Low-redshift SNe only		
	χ^2/dof	GoF (%)	ΔAIC	χ^2/dof	GoF (%)	ΔAIC	χ^2/dof	GoF (%)	ΔAIC
$1/(1+z)$	27.0/35	83.2	0	3.6/13	99.5	0	23.4/22	38.2	0
$1/(1+z)^b$	26.9/34	80.2	1	3.4/12	99.2	1	20.3/21	50.0	-1
tired light	150.3/35	0.0	123	123.4/13	0.0	119	26.9/22	21.4	3

[a] The best-fit values for the b exponent in the second model are as follows. All SNe: $b = 0.97 \pm 0.10$; high-redshift SNe only: $b = 0.95 \pm 0.10$; low-redshift SNe only: $b = 3.18 \pm 1.28$

tween spectra of low- and high-redshift SNe Ia in our sample are small.

We also test for alternate dependencies of the aging rate on redshift, namely $1/(1+z)^b$, although these are not predicted by any model. Whether we consider the entire sample or only the high-redshift sample, the best-fit value for the b exponent is consistent with $b = 1$, and thus with the expected $1/(1+z)$ factor.

That these data provide a confirmation of the time-dilation factor expected in an expanding universe should be of no surprise. Nonetheless, previous use of SN Ia light curves to test this hypothesis (Leibundgut et al. 1996; Goldhaber et al. 2001) are prone to the spread in intrinsic light-curve widths and its possible variation with redshift (which includes selection effects; see Section 1).

The data presented here are unique in that they enable the most direct test of the $1/(1+z)$ time-dilation hypothesis over a larger redshift range than has yet been performed. This hypothesis is favored beyond doubt over models that predict no time dilation. With more data, the focus will shift to testing more thoroughly the alternative $1/(1+z)^b$ dependence of the aging rate on redshift. Any significant deviation from $b = 1$ would have a profound impact on our assumption of a FLRW cosmology to describe the universal expansion.

The authors wish to thank the Supernova Legacy Survey (SNLS) collaboration, and in particular Stéphane Basa and Tianmeng Zhang, for providing spectra of supernova 04D2an prior to publication. The ESSENCE survey is supported by the US National Science Foundation (NSF) through grants AST 04-43378 and AST 05-07475. Support for supernova research at Harvard University, including the CfA Supernova Archive, is provided in part by NSF grant AST 06-06772. The Dark Cosmology Centre is funded by the Danish National Research Foundation. A. C. acknowledges the support of CONICYT, Chile, under grants FONDECYT 1051061 and FONDAP 15010003. T. M. D. appreciates the support of the Villum Kann Rasmussen Fonden. A. V. F. is grateful for the support of NSF grant AST 06-07894. G. P. acknowledges the support of the Proyecto FONDECYT 3070034.

Facilities: VLT:Kueyen (FORS1), VLT:Antu (FORS2), Gemini:South (GMOS), Gemini:Gillete (GMOS), Keck:I (LRIS), Keck:II (DEIMOS, ESI), Magellan:Baade (IMACS), Magellan:Clay (LDSS3).

APPENDIX

A. TIME DILATION IN AN EXPANDING UNIVERSE

In a homogeneous, isotropic expanding universe, the interval $d\tau$ between two space-time events is given by the Robertson-Walker (RW) metric (Robertson 1935, 1936a,b; Walker 1936),

$$d\tau^2 = c^2 dt^2 - a^2(t)\left[\frac{dr^2}{1-kr^2} + r^2(d\theta^2 + \sin^2\theta d\phi^2)\right], \tag{A1}$$

where c is the speed of light in vacuum, t is the cosmic time, (r, θ, ϕ) are the comoving spatial coordinates, k is the curvature parameter, and $a(t)$ is the dimensionless scale factor. In what follows we assume the present-day value of the dimensionless scale factor $a_0 = 1$.

Photons travel along null geodesics ($d\tau^2 = 0$). In what follows we consider radial null rays only ($d\theta = d\phi = 0$). For a photon emitted at time t_1 from an object located at (r_1, θ_1, ϕ_1) and observed at time t_0, Eq. [A1] implies

$$\int_{t_1}^{t_0} \frac{cdt}{a(t)} = \int_0^{r_1} \frac{dr}{\sqrt{1-kr^2}} \equiv f(r_1). \tag{A2}$$

Here we assume that the object from which the photon was emitted has constant coordinates (r_1, θ_1, ϕ_1) such that $f(r_1)$, also known as the comoving distance, is time independent. Thus, for a photon emitted at time $t_1 + \delta t_1$ and observed at time $t_0 + \delta t_0$, Eq. [A1] also implies

$$\int_{t_1+\delta t_1}^{t_0+\delta t_0} \frac{cdt}{a(t)} = f(r_1). \tag{A3}$$

For small δt_1 (and hence small δt_0), the rate of change of the scale factor remains roughly constant and Eqs. [A2] and [A3] imply

$$\frac{\delta t_0}{a_0} = \frac{\delta t_1}{a(t_1)}. \tag{A4}$$

Hence, a light signal emitted with frequency ν_1 will reach us with frequency ν_0 such that

$$\frac{\nu_0}{\nu_1} = \frac{\delta t_1}{\delta t_0} = \frac{a(t_1)}{a_0}. \tag{A5}$$

Using the standard definition of redshift, $z = (l_0 - l_1)/l_1 = \nu_1/\nu_0 - 1$, we obtain a relationship between observed and rest-frame time intervals in a RW metric as a function of redshift z:

$$\frac{\delta t_0}{\delta t_1} = 1 + z. \tag{A6}$$

A supernova at redshift z will thus appear to age $(1 + z)$ times more slowly with respect to a local event at $z \approx 0$.

The prediction of time dilation proportional to $(1+z)$ is generic to expanding universe models, whether the underlying theory be general relativity (e.g., the Friedmann-Lemaître-Robertson-Walker universe), special relativity (e.g., the Milne Universe), or Newtonian expansion. A point of confusion can occur in the special relativistic case for which the well-known time-dilation factor is given by

$$\gamma_{\rm SR} = \left[1 - \left(\frac{v}{c}\right)^2\right]^{-1/2} \tag{A7}$$

$$= \frac{1}{2}\left(1 + z + \frac{1}{1+z}\right), \tag{A8}$$

which evidently differs from $(1+z)$. Thus it might be assumed that a special relativistic expansion can be distinguished from the FLRW universe using a time-dilation test[27].

This is not the case. Special relativistic expansion of the universe assumes there is an inertial frame that extends to infinity (impossible in the non-empty general relativistic picture) and that the expansion involves objects moving through this inertial frame. The time-dilation factor from Eq. [A8] relates the proper time in the moving emitter's inertial frame (δt_1) to the proper time in the observer's inertial frame (δt_0). To measure this time dilation the observer has to set up a set of synchronized clocks (each at rest in the observer's inertial frame) and take readings of the emitter's proper time as the emitter moves past each synchronized clock. The readings show that the emitter's clock is time dilated such that $\delta t_0 = \gamma_{\rm SR}\delta t_1$.

We do not have this set of synchronized clocks at our disposal when we measure time dilation of supernovae in an expanding universe and therefore Eq. [A8] is not the time dilation we observe. We must also take into account an extra time-dilation factor that occurs because the distance to the emitter (and thus the distance light has to propagate to reach us) is increasing. In the time δt_0 the emitter moves a distance $v\delta t_0$ away from us. The total proper time we observe, $\delta t_{0,\rm tot}$, is δt_0 plus an extra factor describing how long light takes to traverse this extra distance $(v\delta t_0/c)$,

$$\delta t_{0,\rm tot} = \delta t_0(1 + v/c). \tag{A9}$$

The relationship between proper time at the emitter and proper time at the observer is thus

$$\delta t_{0,\rm tot} = \gamma_{\rm SR}\delta t_1(1 + v/c) \tag{A10}$$

$$= \delta t_1\sqrt{\frac{1 + v/c}{1 - v/c}} \tag{A11}$$

$$= \delta t_1(1 + z), \tag{A12}$$

which is identical to the GR time-dilation equation.

Non-cosmological redshifts (i.e., not due to universal expansion) also cause a time-dilation effect described by Eq. [A6]. However, these additional effects from peculiar velocities and gravitational redshifts contribute random error only, and do not bias the measurements presented here.

B. COMPARISON OF SPECTRAL AND LIGHT-CURVE AGES

To test the accuracy of the age determination using SNID, we select the SNe Ia for which a well-sampled light curve is available around maximum light. Only the ESSENCE and SNLS SNe Ia in our sample have associated light curves for which we could determine the date of maximum brightness ($t_{\rm max}$). To do so we used the MLCS2k2 light-curve fitting code of Jha et al. (2007), as done by Wood-Vasey et al. (2007). This way we can determine the time difference (in the *observer* frame) between maximum light ($t_{\rm max}$) and the time the spectrum was obtained ($t_{\rm obs}$). We compare this time interval with the *rest-frame* age determined through cross-correlation with local SN Ia spectral templates using SNID ($t_{\rm spec}$). We expect a one-to-one correspondence between

$$t_{\rm LC} = \frac{t_{\rm obs} - t_{\rm max}}{1 + z} \tag{B1}$$

[27] In fact, such an erroneous assumption was made by one of the current authors of Davis & Lineweaver (2004).

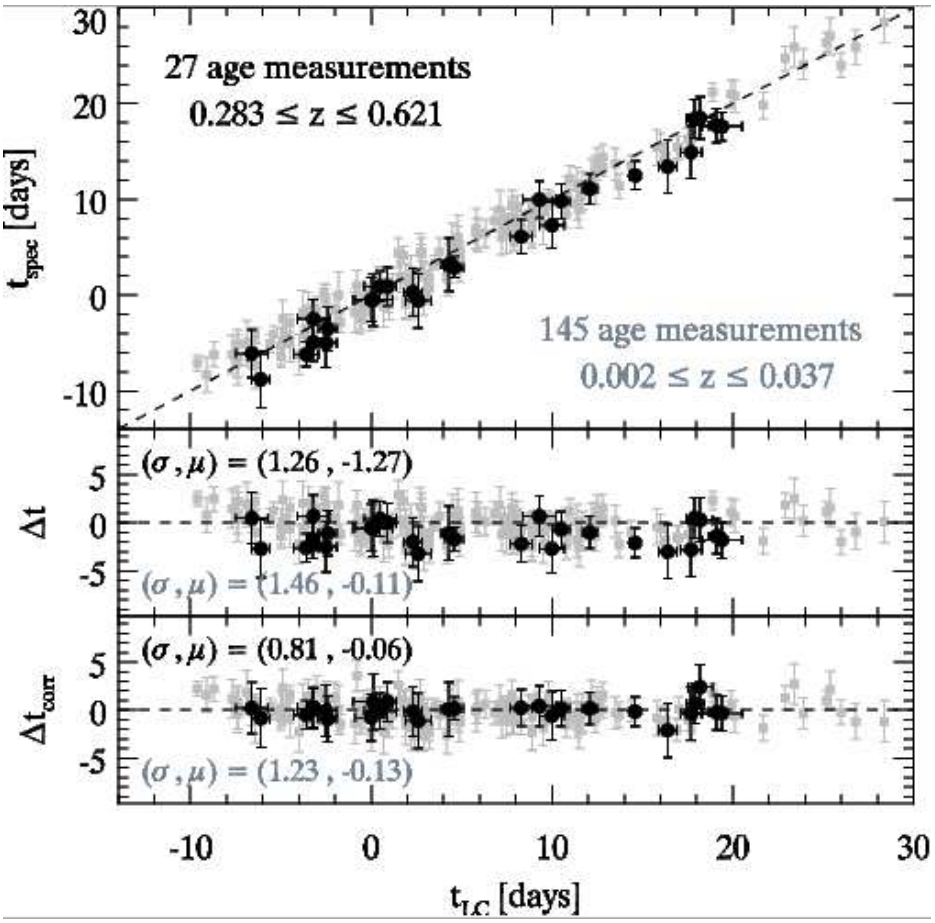

FIG. 10.— Upper panel: comparison of supernova *rest-frame* ages (in days from maximum light) obtained from cross-correlation with spectral templates ($t_{\rm spec}$) and from fits to the light curve ($t_{\rm LC}$). 145 age measurements for the subsample of 22 low-redshift SNe Ia are shown in gray. The dashed line represents the one-to-one correspondence between $t_{\rm LC}$ and $t_{\rm spec}$. Middle panel: Age residuals, $\Delta t = t_{\rm spec} - t_{\rm LC}$. We also indicate the standard deviation (σ) and mean residual (μ). Lower panel: Same as above, where each point has been corrected for the mean offset between $t_{\rm spec}$ and $t_{\rm LC}$ for a given supernova.

and $t_{\rm spec}$.

The result is shown as black points in Fig. 10. While the agreement is good, there is a mean systematic offset of -1.6 d between $t_{\rm spec}$ and $t_{\rm LC}$, as shown in the middle panel. If this offset were to affect only a subset of age measurements for a given supernova, the impact on the aging rate determination would be severe. To check this, we correct the spectral ages of a given supernova for the mean difference between $t_{\rm LC}$ and $t_{\rm spec}$. This "corrected" age residual, $\Delta t_{\rm corr}$ is plotted in the lower panel of Fig. 10. The mean residual drops to -0.1 d and the scatter decreases slightly.

Since there are 2 to 4 $t_{\rm spec}$ measurements for a given supernova, and only one measurement of $t_{\rm max}$, the source of the discrepancy between the spectral and light-curve ages is most likely due to the determination of the date of maximum using the light-curve fitter. Indeed, using a different light-curve fitter (SALT2; Guy et al. 2007) yields values for $t_{\rm max}$ that differ from the MLCS2k2 measurements by more than one day in 9 out of 10 cases, and by more than two days for three objects (SNe 2003js, 2007tg, and 2007un). These discrepancies are due to a combination of differences in light-curve fitter algorithms and data quality (light-curve sampling around maximum light and signal-to-noise ratio of each light-curve measurement; see Miknaitis et al. 2007).

Therefore, while there is a systematic offset between part of these different age determinations, this offset affects all measurements in a similar fashion and has no impact on the determination of the *rate* of aging. In fact, the main result of this paper (see Section 4) is completely independent of $t_{\rm LC}$, and hence of $t_{\rm max}$. Nonetheless, the comparison between spectral and light-curve ages confirms the accuracy of age determination using spectra alone (Blondin & Tonry 2007). The age measurements for all the high-redshift SNe Ia in our sample are reported in Table 5.

In making the comparison we have implicitly assumed what we are trying to show, namely a time-dilation factor of $(1+z)$. Accordingly, we also make the same comparison for our subsample of 22 low-redshift SNe Ia ($0.002 \leq z \leq 0.04$). At such low redshifts, the $(1+z)$ correction present in $t_{\rm LC}$ is negligible (the mean correction is ~ 0.06 d). The result is shown as gray points in Fig. 10. The mean residual between $t_{\rm LC}$ and $t_{\rm spec}$ for this low-redshift sample is close to zero with a small scatter ($\sigma \approx 1.5$ d), and unlike the high-redshift sample there is no significant systematic offset between the two age measurements.

The age measurements presented in Table 2 also enable us to infer the date of maximum light for each supernova using spectra alone (corresponding to $t_{\rm spec} = 0$). This way we are able to determine the time of maximum for the SNe Ia in our sample for which a well-sampled light curve was unavailable (SNe 1996bj, 1997ex, and 2001go; see Table 6). We

TABLE 5
Comparison of rest-frame light-curve and spectral ages

SN (1)	$t_{\rm LC}$ (2)	$t_{\rm spec}$ (3)	Δt (4)	$\Delta t_{\rm corr}$ (5)
2002iz	0.1 (1.1)	−0.5 (2.2)	−0.6 (2.4)	0.8 (1.5)
	19.4 (1.1)	17.6 (1.2)	−1.8 (1.6)	−0.4 (2.3)
b027	−2.4 (0.5)	−3.5 (1.8)	−1.1 (1.9)	−0.9 (1.7)
	17.9 (0.5)	18.4 (1.6)	0.5 (1.7)	0.7 (1.4)
2003js	−3.2 (0.3)	−4.9 (1.6)	−1.7 (1.6)	0.3 (2.0)
	14.6 (0.3)	12.5 (1.2)	−2.1 (1.2)	−0.1 (2.3)
04D2an	−3.2 (0.9)	−2.5 (1.6)	0.7 (1.8)	0.2 (1.4)
	0.5 (0.9)	0.9 (1.3)	0.4 (1.6)	−0.1 (1.3)
2006mk	−3.6 (0.7)	−6.2 (1.0)	−2.6 (1.3)	−0.5 (2.7)
	2.6 (0.7)	−0.6 (2.2)	−3.2 (2.3)	−1.1 (3.3)
	10.0 (0.7)	7.3 (1.9)	−2.7 (2.0)	−0.6 (2.8)
	18.2 (0.7)	18.5 (1.8)	0.3 (1.9)	2.4 (0.9)
2006sc	0.9 (0.5)	0.9 (1.6)	0.0 (1.7)	0.9 (1.0)
	10.5 (0.5)	9.8 (1.4)	−0.7 (1.5)	0.2 (1.2)
	16.4 (0.5)	13.4 (2.2)	−3.0 (2.3)	−2.1 (3.2)
2006tk	−6.1 (0.5)	−8.8 (2.4)	−2.7 (2.5)	−0.8 (2.8)
	2.3 (0.5)	0.3 (2.0)	−2.0 (2.1)	−0.1 (2.2)
	4.6 (0.5)	2.9 (0.9)	−1.7 (1.0)	0.2 (1.9)
2007tg	−6.6 (0.9)	−6.1 (2.0)	0.5 (2.2)	0.2 (1.2)
	0.0 (0.9)	−0.5 (1.8)	−0.5 (2.0)	−0.8 (1.2)
	9.3 (0.9)	10.0 (1.5)	0.7 (1.8)	0.4 (1.3)
2007tt	−2.5 (0.6)	−5.0 (2.1)	−2.5 (2.2)	−0.1 (2.7)
	8.3 (0.6)	6.1 (1.4)	−2.2 (1.6)	0.2 (2.5)
	17.7 (0.6)	14.9 (2.2)	−2.8 (2.2)	−0.4 (3.0)
2007un	4.3 (0.4)	3.2 (2.2)	−1.1 (2.3)	0.1 (1.4)
	12.1 (0.4)	11.1 (1.3)	−1.0 (1.3)	0.2 (1.4)
	19.1 (0.4)	17.7 (1.4)	−1.4 (1.5)	−0.2 (1.7)

Column headings: (1) SN name. (2) SN rest-frame age in days from maximum light, derived from the light curve. (3) SN rest-frame age in days from maximum light, derived from the cross-correlation with spectral templates using SNID. (4) $\Delta t = t_{\rm spec} - t_{\rm LC}$. (5) Δt corrected for the mean offset between $t_{\rm spec}$ and $t_{\rm LC}$.

TABLE 6
Comparison of dates of maximum light

SN (1)	$t_{\rm max}^{\rm LC}$ (2)	$t_{\rm max}^{\rm spec}$ (3)	$\Delta t_{\rm max}$ (4)
1996bj	···	372.16 (3.73)	···
1997ex	···	817.16 (1.98)	···
2001go	···	2011.47 (3.12)	···
2002iz	2586.83 (1.51)	2587.71 (3.21)	0.88 (3.54)
b027	2593.09 (0.65)	2594.20 (1.90)	1.11 (2.01)
2003js	2946.80 (0.47)	2949.29 (1.67)	2.49 (1.73)
04D2an	3031.36 (1.50)	3030.61 (1.82)	−0.75 (2.36)
2006mk	4036.95 (0.96)	4040.32 (1.02)	3.37 (1.40)
2006sc	4062.39 (0.64)	4061.71 (2.77)	−0.68 (2.84)
2006tk	4097.56 (0.66)	4100.13 (0.98)	2.57 (1.18)
2007tg	4391.62 (1.34)	4391.34 (1.58)	−0.28 (2.08)
2007tt	4419.29 (0.83)	4422.47 (1.83)	3.18 (2.01)
2007un	4436.12 (0.47)	4437.15 (3.12)	1.03 (3.16)

Column headings: (1) SN name. (2) JD − 2,450,000 of maximum light, derived from the light curve. (3) JD − 2,450,000 of maximum light, derived from the spectra. (4) $\Delta t_{\rm max} = t_{\rm max}^{\rm spec} - t_{\rm max}^{\rm LC}$.

can also compare the dates of maximum as inferred from a fit to the light curve ($t_{\rm max}^{\rm LC}$) with those determined from the spectra alone ($t_{\rm max}^{\rm spec}$). The results are also shown in Table 6. For four objects (SNe 2003js, 2006mk, 2006tk, and 2007tt) the disagreement is larger than 1σ, and explains the systematic negative offset between $t_{\rm spec}$ and $t_{\rm LC}$ seen in Fig. 10.

REFERENCES

Akaike, H. 1974, IEEE Transactions on Automatic Control, 19, 716
Benetti, S., et al. 2005, ApJ, 623, 1011
Blondin, S., et al. 2006, AJ, 131, 1648
Blondin, S. & Tonry, J. L. 2007, ApJ, 666, 1024
Conley, A., et al. 2006, AJ, 132, 1707

Davis, T. M. & Lineweaver, C. H. 2004, Publications of the Astronomical Society of Australia, 21, 97
Davis, T. M., et al. 2007, ApJ, 666, 716
Falco, E. E., et al. 1999, PASP, 111, 438
Foley, R. J., Filippenko, A. V., Leonard, D. C., Riess, A. G., Nugent, P., & Perlmutter, S. 2005, ApJ, 626, L11
Goldhaber, G., et al. 2001, ApJ, 558, 359
Guy, J., et al. 2007, A&A, 466, 11
Hamuy, M., Phillips, M. M., Maza, J., Suntzeff, N. B., Schommer, R. A., & Aviles, R. 1995, AJ, 109, 1
Hamuy, M., et al. 2003, Nature, 424, 651
Hicken, M., Garnavich, P. M., Prieto, J. L., Blondin, S., DePoy, D. L., Kirshner, R. P., & Parrent, J. 2007, ApJ, 669, L17
Hook, I. M., et al. 2005, AJ, 130, 2788
Howell, D. A., Sullivan, M., Conley, A., & Carlberg, R. 2007, ApJ, 667, L37
Howell, D. A., et al. 2006, Nature, 443, 308
Howell, D. A., et al. 2005, ApJ, 634, 1190
Jha, S., Riess, A. G., & Kirshner, R. P. 2007, ApJ, 659, 122
Leibundgut, B., et al. 1996, ApJ, 466, L21
Li, W., et al. 2003, PASP, 115, 453
Li, W., et al. 2001a, PASP, 113, 1178
Li, W., Filippenko, A. V., Treffers, R. R., Riess, A. G., Hu, J., & Qiu, Y. 2001b, ApJ, 546, 734
Liddle, A. R. 2004, MNRAS, 351, L49
Lidman, C., et al. 2005, A&A, 430, 843
Matheson, T., et al. 2005, AJ, 129, 2352
Matheson, T., et al. 2008, accepted for publication in AJ
Mazzali, P. A., Sauer, D. N., Pastorello, A., Benetti, S., & Hillebrandt, W. 2008, ArXiv e-prints, 803
Miknaitis, G., et al. 2007, ApJ, 666, 674
Nomoto, K., Thielemann, F.-K., & Yokoi, K. 1984, ApJ, 286, 644
Nugent, P., Phillips, M., Baron, E., Branch, D., & Hauschildt, P. 1995, ApJ, 455, L147+
Phillips, M. M. 1993, ApJ, 413, L105
Phillips, M. M., Lira, P., Suntzeff, N. B., Schommer, R. A., Hamuy, M., & Maza, J. 1999, AJ, 118, 1766
Pinto, P. A. & Eastman, R. G. 2000, ApJ, 530, 757
Riess, A. G., et al. 1997, AJ, 114, 722
Riess, A. G., et al. 1999, AJ, 118, 2675
Riess, A. G., Press, W. H., & Kirshner, R. P. 1995, ApJ, 438, L17
Robertson, H. P. 1935, ApJ, 82, 284
—. 1936a, ApJ, 83, 187
—. 1936b, ApJ, 83, 257
Rust, B. W. 1974, PhD thesis, Oak Ridge National Lab., TN.
Stehle, M., Mazzali, P. A., Benetti, S., & Hillebrandt, W. 2005, MNRAS, 360, 1231
Stritzinger, M. 2005, PhD thesis, Technische Universität München,
Tonry, J. & Davis, M. 1979, AJ, 84, 1511
Walker, A. G. 1936, in Proceedings of the London Mathematical Society, 90–127
Weinberg, S. 1972, Gravitation and Cosmology: Principles and Applications of the General Theory of Relativity (Gravitation and Cosmology: Principles and Applications of the General Theory of Relativity, by Steven Weinberg, pp. 688. ISBN 0-471-92567-5. Wiley-VCH , July 1972.)
Wilson, O. C. 1939, ApJ, 90, 634
Wood-Vasey, W. M., et al. 2007, ApJ, 666, 694
Zwicky, F. 1929, Proceedings of the National Academy of Science, 15, 773